PHYSICAL REVIEW B **84**, 045104 (2011)

Valence transition in (Pr,Ca)CoO_3 cobaltites: Charge migration at the metal-insulator transition

José Luis García-Muñoz,[1,*] Carlos Frontera,[1] Aura J. Barón-González,[1] Sergio Valencia,[2] Javier Blasco,[3] Ralf Feyerherm,[2] Esther Dudzik,[2] Radu Abrudan,[4] and Florin Radu[2]

[1]*Institut de Ciència de Materials de Barcelona, ICMAB-CSIC, Campus universitari de Bellaterra, E-08193 Bellaterra, Barcelona, Spain*
[2]*Helmholtz-Zentrum Berlin, Albert-Einstein-Strasse 15, D-12489 Berlin, Germany*
[3]*Instituto de Ciencias de Materiales de Aragón, CSIC-Universidad de Zaragoza, c/ Pedro Cerbuna 12, E-50009 Zaragoza, Spain*
[4]*Institut für Experimentalphysik/Festkörperphysik, Ruhr-Universität Bochum, D-44780 Bochum, Germany*

(Received 16 August 2010; revised manuscript received 21 March 2011; published 5 July 2011)

X-ray absorption spectroscopy measurements in $Pr_{0.5}Ca_{0.5}CoO_3$ and $(Pr,Y)_{0.55}Ca_{0.45}CoO_3$ compositions reveal that the valence of praseodymium ions is stable and essentially +3 (Pr [$4f^2$]) in the metallic state, but abruptly changes when carriers localize approaching the oxidation state +4 (Pr [$4f^1$]). This mechanism appears to be the driving force of the metal-insulator transition. The ground insulating state of $Pr_{0.5}Ca_{0.5}CoO_3$ is a homogeneous $Co^{3.5-\delta}$ state stabilized by a charge transfer from Pr to Co sites: $\frac{1}{2}\,Pr^{3+} + Co^{3.5} \rightarrow \frac{1}{2}\,Pr^{3+2\delta} + Co^{3.5-\delta}$, with $2\delta \approx 0.26e^-$.

DOI: 10.1103/PhysRevB.84.045104 PACS number(s): 71.30.+h, 75.25.Dk, 75.30.Wx, 78.70.Dm

I. INTRODUCTION

Co oxides are attracting much attention in the condensed matter community as they present a rich variety of interesting phenomena.[1–5] Spin-state transitions in oxides having Co^{3+} ions is one of the most celebrated.[6–10] Different types of metal-insulator transitions (MITs) are being investigated in Ln-A-Co-O (Ln: lanthanide; A: alkaline earth) cobaltites having in common CoO_6 octahedra with a small energy difference between crystal-field splitting and Hund's coupling energy.[11–14]

Ln-*A*-Co-O oxides offer new frameworks to obtain remarkable magnetic and transport properties (for applications in the field of electronics) due to the ability of Co to adopt various oxidation states and electronic configurations. $Pr_{0.5}Ca_{0.5}CoO_3$ exhibits a MIT ($T_{MI} = 70$ K) and is considered a "strongly correlated spin-crossover" system.[12,14] Recent experiments have proved the possibility of generating metallic domains in the insulating low-temperature phase of $Pr_{0.5}Ca_{0.5}CoO_3$ by ultrafast photoexcitation, making this material of interest in the area of ultrafast optical switching devices.[15] The ionic description of the $t_{2g}^5(\sigma^*)^{0.5}$ metallic state involves the coexistence of intermediate-spin (IS) Co^{3+} ($S = 1$, $t_{2g}^5 e_g^1$) and low-spin (LS) Co^{4+} ($S = 1/2$, t_{2g}^5) mobile species. Both ionic configurations are Jahn-Teller active and might require the creation of local lattice distortions in the localized state. A spin-state transition from IS Co^{3+} to diamagnetic LS Co^{3+} and a charge ordering of Co^{3+} ($S = 0$, t_{2g}^6) and Co^{4+} sites was proposed as the origin of the MIT transition.[12] The first is widely accepted, but charge ordering with two differentiated $Co^{3.5-\delta}$ and $Co^{3.5+\delta}$ sites has not been detected.

Several works have reported similar MITs in $(Pr_{1-y}Ln_y)_{1-x}Ca_xCoO_3$ (Ln: Sm, Tb, Y, ...) perovskites for different Ca contents ($x = 0.3, 0.4, 0.5$, etc.).[16–18] The existence of the MIT depends not only on x, but also on y and the lanthanide species.[18] In these cases it was generally assumed that, besides the effects of temperature and hydrostatic pressure, both x and y parameters have a strong influence on the number of electrons in the e_g orbitals.[17] According to magnetic and transport measurements, the transition was viewed as a sudden IS $\rightarrow$ LS transformation of Co^{3+} atoms in the ionic description in some compounds, but also as a more gradual IS$\rightarrow$LS crossover in other compositions.[18]

However, in recent years there has been increasing evidence that the first-order MIT with x close to 0.5 occurs only for (Ln, Ln', Ca) cations with Ln = Pr,[14,17–20] raising speculations about the role played by the Pr-O hybridization on the MIT in these cobaltites. Moreover, a (Pr,Ca)-O bond contraction has been observed across T_{MI}.[20–22]

In this work we present x-ray absorption measurements at the Pr and Co sites revealing that a Pr^{3+}/Pr^{4+} valence transition at T_{MI} is responsible for charge localization, and also acts as the driving force for the stabilization of the Co^{3+} LS state in the insulating phase of $Pr_{0.5}Ca_{0.5}CoO_3$ and related compositions. We provide direct experimental observation of a sudden spontaneous charge migration from Pr to Co sites exactly at the MIT. Electron migration stabilizes the trivalent state of Co in half-doped $Pr_{0.5}Ca_{0.5}CoO_3$. Instead of disordered Co^{3+}/Co^{4+} sites (ionic description) or $Co^{3.5+\delta}/Co^{3.5-\delta}$ sites (charge disproportionation), the actual ground state consists of a homogeneous $Co^{3.5-\delta}$ state ($\delta \approx 0.13e^-$) arising from an electron transfer from praseodymium (electron migration from *A* to *B* sites of the perovskite).

II. EXPERIMENTAL DETAILS

Polycrystalline samples of $Pr_{0.5}Ca_{0.5}CoO_3$, $Pr_{0.55}Ca_{0.45}CoO_3$, and $Pr_{0.50}Y_{0.05}Ca_{0.45}CoO_3$ were prepared as detailed elsewhere.[20] Final sintering of the samples was performed under high oxygen pressure ($p_{O_2} = 200$ bars) to assure optimal oxygen content. Samples were well crystallized and free from impurities as revealed by x-ray and neutron diffraction. Neutron powder diffraction (NPD) data were collected on D2B ($\lambda = 1.594$ Å), D1B ($\lambda = 2.52$ Å), and D20 ($\lambda = 1.88$ Å) diffractometers of ILL (Grenoble). Diffraction patterns were recorded in the temperature range between 5 K and room temperature (RT). Magnetization measurements were performed using a superconducting quantum interference device (SQUID) magnetometer; ac susceptibility, magnetotransport, and thermoelectric power data were recorded using a commercial physical properties measurement system (PPMS) in the temperature range

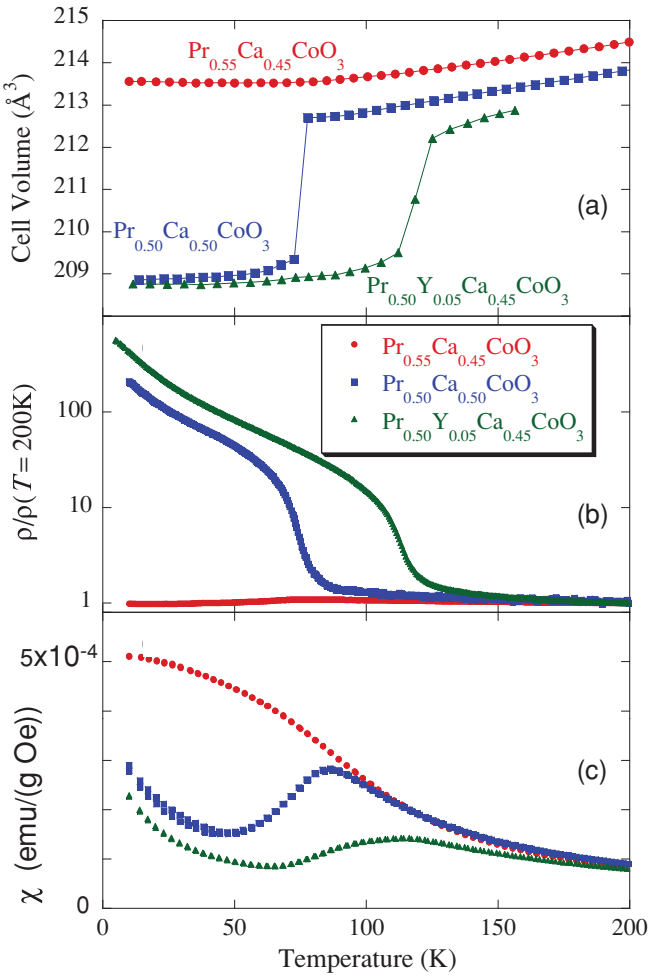

FIG. 1. (Color online) (a) Thermal evolution of the unit-cell volume for $Pr_{0.5}Ca_{0.5}CoO_3$, $Pr_{0.55}Ca_{0.45}CoO_3$, and $Pr_{0.5}Y_{0.05}Ca_{0.45}CoO_3$ obtained from neutron diffraction measurements. The volume contraction indicates the entrance of the insulating phase. It is not present in $Pr_{0.55}Ca_{0.45}CoO_3$ (FM and metallic ground state). (b) Resistivity of the three perovskites plotted in logarithmic scale. (c) Magnetic susceptibility (0.1 T, zero-field cooling or cooling and heating cycle).

$2 < T < 350$ K. Absorption measurements were performed on beam lines MAGS and PM-3 at the BESSY II synchrotron radiation source.[23] X-ray absorption spectra (XAS) were collected by means of bulk-sensitive fluorescence yield (FY). Temperature dependence of the absorption was measured on heating between 10 and 300 K.

III. RESULTS AND DISCUSSION

A. Pr valence change at the metal-insulator transition

Figure 1(a) shows the evolution with temperature of the unit-cell volume of all three compounds as determined from Rietveld refinement of NPD data. $Pr_{0.55}Ca_{0.45}CoO_3$ does not show the characteristic volume contraction with decreasing T associated to the localization of the charges in these systems. This result is consistent with the temperature dependence of the resistivity (ρ) and of the susceptibility (χ) [see Figs. 1(b) and 1(c), respectively] which show that this compound remains metallic even at low temperatures. Moreover, the metallic phase of $Pr_{0.55}Ca_{0.45}CoO_3$ displays long-range FM order below $T_C = 70$ K. On the contrary, both $Pr_{0.5}Ca_{0.5}CoO_3$ and $Pr_{0.50}Y_{0.05}Ca_{0.45}CoO_3$ display a volume cell contraction concomitant with a first-order MIT. The transition to a low-temperature charge-localized state takes place in $Pr_{0.50}Y_{0.05}Ca_{0.45}CoO_3$ at a higher temperature ($T_{MI} = 120$ K) than in the half-doped cobaltite ($T_{MI} = 70$ K). Resistivity data agrees with the opening of a gap and both compounds exhibit semiconductorlike behavior below T_{MI}.

To investigate the role of the Pr cation on the MIT transition x-ray absorption spectra at the Pr L_3 edge have been acquired on MAGS as a function of temperature for all three samples. Absorption spectra have been obtained by means of fluorescence yield (FY-XAS). All spectra are depicted after normalization to their area on Fig. 2. The two main spectroscopic features at 5967 and 5978 eV (respectively, A and B) originate from the Pr $2p \rightarrow 5d$ transitions: Pr^{3+} ($4f^2$) sites contribute to the peak at lower energy, and the Pr^{4+} sites contribution splits over the two peaks due to $4f^1$ and $4f^2\underline{L}$ states, being $\underline{L}$ a ligand hole in the O $2p$ orbital.[24,25] In $Pr_{0.5}Ca_{0.5}CoO_3$ [Fig. 2(a)] the measurements show very apparent changes in the spectra when crossing T_{MI}. The intensity of peak B (Pr^{4+} only contribution, i.e., $4f^1$) increases at the same time as the intensity of peak A (being Pr^{3+} the major contributor, i.e., $4f^2$) decreases. These results reveal a rapid increase of the Pr oxidation state at the transition. Photoabsorption spectra evidence that praseodymium changes to an intermediate valence ground state composed essentially of an atomiclike $4f^1$ state when crossing T_{MI}. A localized $4f^1$ configuration with a degree of covalent mixing should create in the oxygen $2p$ valence band extended states of f symmetry.

The above results highlight the role of the Pr-O hybridization on the MIT. To further confirm this point, Fig. 1(b) shows the Pr L_3 FY-XAS spectra obtained for $Pr_{0.55}Ca_{0.45}CoO_3$ at various temperatures. No relevant spectroscopic changes are seen in this case pointing to a temperature-independent oxidation state of Pr. This agrees with the fact that no MIT is seen in such compositions.

B. Tilting of the CoO_6 octahedra and the occurrence of the Pr $4f^2 \rightarrow 4f^1$ transition: Pr-O hybridization investigated by neutron diffraction

The persistence of the metallic state in $Pr_{0.55}Ca_{0.45}CoO_3$ is related to the degree of the $GdFeO_3$-type distortion. The *Pnma* structure of $Pr_{0.55}Ca_{0.45}CoO_3$ is less distorted than $Pr_{0.5}Ca_{0.5}CoO_3$. From our NPD data one obtains the following Co-O-Co bond angles: θ_1[Co-O(1)-Co] = 159.0(1)° and θ_2[Co-O(2)-Co] = 157.76(1)° at RT in metallic $Pr_{0.55}Ca_{0.45}CoO_3$. This distortion should be compared with $\theta_1 = 158.18(3)°$ and $\theta_2 = 157.95(6)°$ in $Pr_{0.5}Ca_{0.5}CoO_3$. Although the θ_2 values are approximately equal (slightly greater for the half-doped cobaltite), the apical bonding angle θ_1 is straighter by ≈1° in $Pr_{0.55}Ca_{0.45}CoO_3$.

Table I illustrates the decisive importance of the apical tilting of the octahedra (θ_1) for the activation of the $4f^2/4f^1$ electronic transition. In this table we compare the bond lengths between A-site (Pr,Ca) and O atoms at both sides

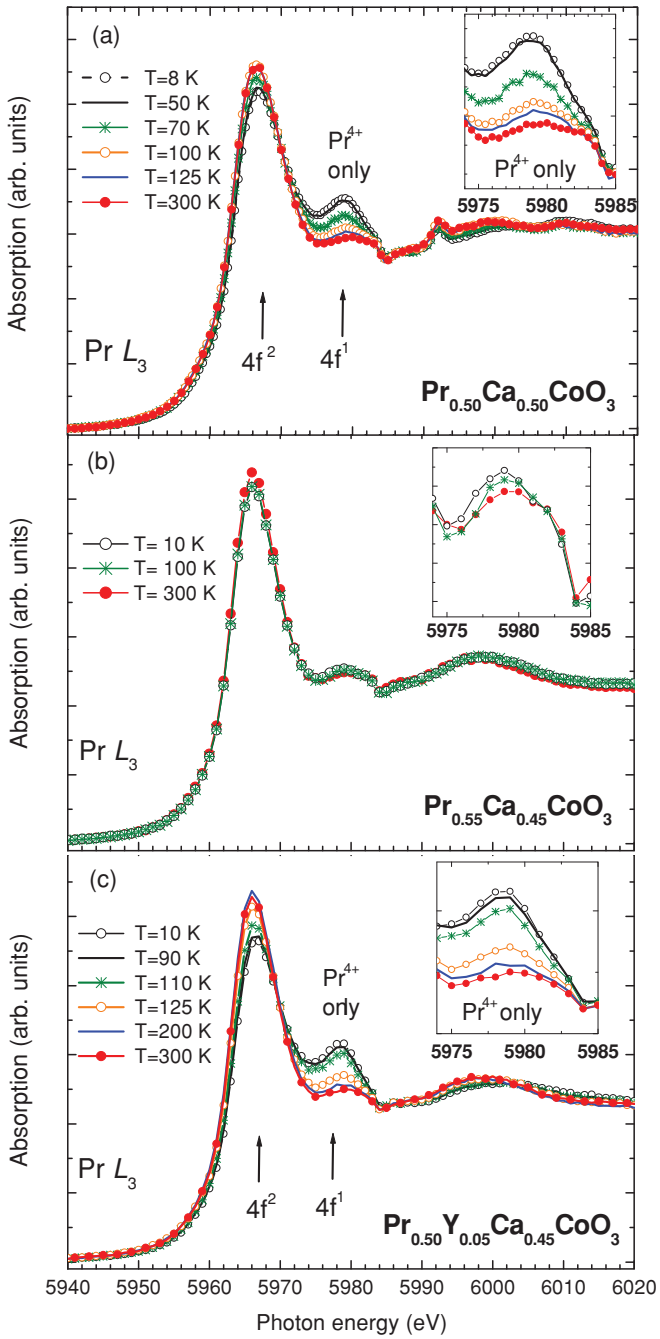

FIG. 2. (Color online) Temperature dependence of the Pr L_3-edge FY-XAS of (a) $Pr_{0.5}Ca_{0.5}CoO_3$, (b) $Pr_{0.55}Ca_{0.45}CoO_3$ (metallic at all temperatures), and (c) $Pr_{0.5}Y_{0.05}Ca_{0.45}CoO_3$. Insets: enlarged $4f^1$ region.

of the metal-insulator transition in $Pr_{0.5}Ca_{0.5}CoO_3$. Each praseodymium is bonded to 12 oxygens: eight basal oxygens at 8*d* general position (Pr-O2 bonds), and four apical oxygens at 4*c* positions (Pr-O1). The two strongest Pr-O bond contractions ($\approx -2.4\%$) at the MIT involve apical oxygens (Pr-O1). Pr-O1 bonds are parallel to the *a*-*c* plane because Pr and O1 atoms both occupy 4*c* positions (x 1/4 z), at the same y layer. Both atoms considerably shift their positions in the plane varying the tilting angle $\phi_1 = 1/2(180^\circ - \theta_1)$ of the octahedra. The angles θ_1 and θ_2 change by $\approx 3^\circ$ on cooling

TABLE I. Refined A-O bond lengths in $Pr_{0.5}Ca_{0.5}CoO_3$ and relative variation across the metal-insulator transition due to Pr^{3+}/Pr^4 valence change. The *A* site is occupied by [Pr,Ca] atoms.

$Pr_{0.5}Ca_{0.5}CoO_3$	10 K insulator	Relative variation 10–100 K	100 K metal	300 K metal
A-O1 (Å)	2.286(3)	−2.36%	2.340(3)	2.380(3)
A-O1 (Å)	2.396(2)	−2.38%	2.453(2)	2.475(2)
A-O2 (Å) *x*2	2.306(2)	−2.08%	2.354(2)	2.344(2)
A-O2 (Å) *x*2	2.538(2)	−1.22%	2.569(2)	2.585(2)
A-O2 (Å) *x*2	2.591(2)	−1.00%	2.617(2)	2.630(2)
$\langle d_{A-O}\rangle_{8-short}$ (Å)	2.444		2.484	2.497
A-O1 (Å)	3.009(2)	+2.29%	2.940(2)	2.921(2)
A-O1 (Å)	3.015(3)	+0.50%	3.000(3)	3.013(3)
A-O2 (Å) *x*2	3.229(2)	+1.79%	3.171(2)	3.139(2)
$\langle d_{A-O}\rangle_{4-long}$ (Å)	3.120		3.070	3.053

across the transition.[20–22] The change $\Delta\theta_1$ is the main cause of opposite spatial shifts of Pr and O1 atoms within the *a*-*c* plane: $u_x = 0.0079$, $u_z = -0.0023$ and $|s| = 0.044$ Å for Pr, and $u_x = -0.0044$, $u_z = 0.0097$, and $|s| = 0.0567$ Å for O1, where u_i are the relative and $|s|$ the total displacements.

To get further insight on the decisive importance of the tilting of the CoO_6 octahedra for the occurrence of the $4f^2 \rightarrow 4f^1$ transition we compare the above results with those obtained for $Pr_{0.50}Y_{0.05}Ca_{0.45}CoO_3$. In that case the substitution of 5% of Y atoms, of smaller size than Pr and Ca, increases the tilting of the octahedra. From NPD we obtain $\theta_1 = 157.56(1)^\circ$ and $\theta_2 = 157.67(1)^\circ$ at RT. The basal angle θ_2 is almost identical to metallic $Pr_{0.55}Ca_{0.45}CoO_3$ but the apical angle θ_1 is $\approx 1.5^\circ$ smaller. The Pr L_3 FY-XAS spectra for this sample [Fig. 1(c)] indeed show, as for $Pr_{0.50}Ca_{0.50}CoO_3$, a very clear evolution where the Pr^{4+} contribution increases below $\approx$130 K. In this case the tilting angle ϕ_1 brings the apical oxygen O1 nearer to some Pr atom at the $y = 1/4$ layer. Moreover, ϕ_1 tilts the basal plane $CoO2_4$ of the octahedron towards a more vertical position moving the basal oxygens O2 towards the up ($y = 1/4$) and down ($y = 3/4$) Pr planes.

C. Pr^{3+}/Pr^{4+} and $Co^{3.5+}/Co^{3+}$ valence shifts: Electron migration from Pr to Co at T_{MI}

The absorption data at ambient temperature indicate an essentially trivalent Pr in all cases.[25,26] Electronic-structure calculations reported by Kníže k *et al.* indicated a certain Pr(4*f*)-O(2*p*) hybridization already in metallic $Pr_{0.5}Ca_{0.5}CoO_3$ that produces a broadband 0.5 eV below Fermi level, much broader than the corresponding Nd(4*f*) band in $Nd_{0.5}Ca_{0.5}CoO_3$.[14] Although a precise determination of the Pr valence would require very specific theoretical calculations, we have parametrized the valence changes monitored in the FY-XAS data from the intensity changes in the spectroscopic features at 5967 eV (*A*) and 5978 eV (*B*). As in some previous XAS studies of L_3 edges (e.g., Yamaoka *et al.*[25] and Richter *et al.*[26]), the changes in Pr valence are estimated from the relative ratio of intensities corresponding to *A* and *B* spectral features, i.e., I_A/I_B.[26] Both I_A and I_B were obtained by fitting the spectra with two Voigt functions after subtracting the

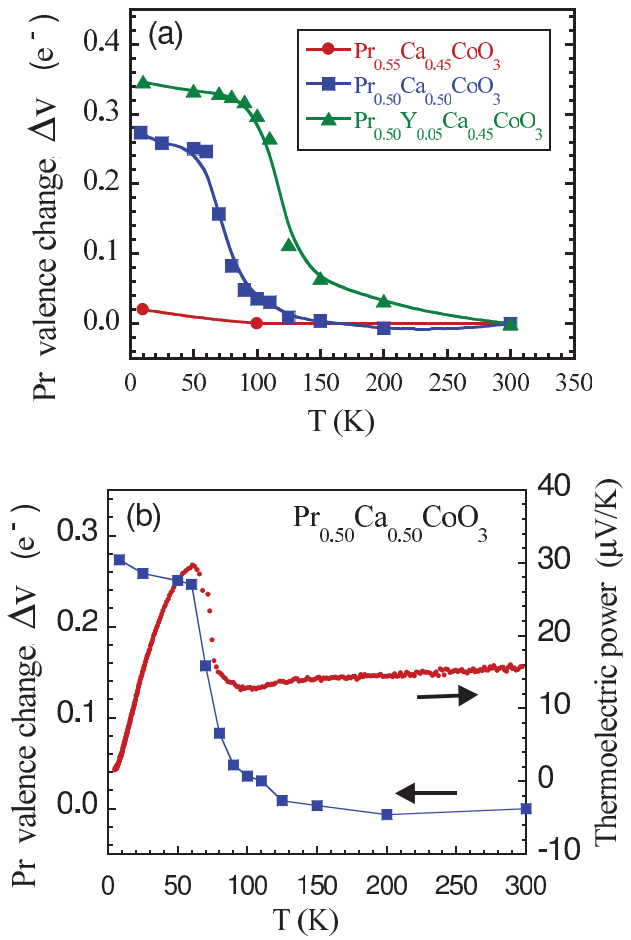

FIG. 3. (Color online) (a) Evolution of the valence change of praseodymium (in reference to RT, simply estimated as described in the text) across the MIT in $Pr_{0.5}Ca_{0.5}CoO_3$ and $Pr_{0.5}Y_{0.05}Ca_{0.45}CoO_3$, and in metallic $Pr_{0.55}Ca_{0.45}CoO_3$. The solid lines are guides to the eye. (b) Comparison of the thermal dependences of the Pr valence change and the Seebeck coefficient in $Pr_{0.5}Ca_{0.5}CoO_3$.

steplike signal from the continuum. Undefined T-independent contribution of extended x-ray-absorption fine structure to the intensity of the B feature avoids exact quantification of the Pr valence,[27] however, a simple estimation of the change of the Pr valence (Δv[Pr]) with respect to its value at RT is feasible. The changes Δv[Pr] estimated for all three compositions are plotted in Fig. 3(a) as temperature decreases. Decreasing temperature, between RT and T_{MI}, the system keeps its metallic state and according to Fig. 3(a) the valence of Pr in $Pr_{0.5}Ca_{0.5}CoO_3$ remains constant. As the temperature approaches T_{MI}, the Pr valence in Fig. 3(a) rapidly increases and the estimated change is $\Delta v[\mathrm{Pr}] \approx 0.26(2)e^-$. A broader but similar transition is observed in $Pr_{0.50}Y_{0.05}Ca_{0.45}CoO_3$ ($\Delta v[\mathrm{Pr}] \approx 0.28(3)e^-$). The evolution below RT corresponding to metallic $Pr_{0.55}Ca_{0.45}CoO_3$ is also shown in Fig. 3(a). This compound does not show appreciable changes in the electronic configuration of Pr.

Figure 3(b) displays a comparison of the electron migration from Pr sites as obtained from absorption measurements with the Seebeck coefficient (α) as a function of temperature for $Pr_{0.5}Ca_{0.5}CoO_3$. This figure clearly illustrates that changes in

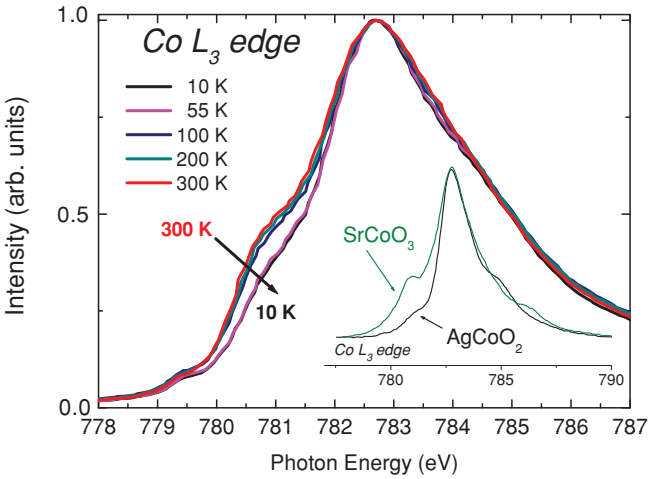

FIG. 4. (Color online) Co L_3-edge spectra of $Pr_{0.5}Ca_{0.5}CoO_3$ across the transition. The RT spectra of $SrCoO_3$ and $AgCoO_2$ (Ref. 30) are shown for comparison.

the oxidation state of praseodymium are perfectly simultaneous to changes in the Seebeck coefficient. At RT we obtain a Seebeck coefficient $\alpha \approx +15\ \mu$V/K. On cooling, the linear metallic behavior of $\alpha(T)$ ends with a sharp increase (reaching $+30\ \mu$V/K) when a fraction of electrons with $4f$ symmetry start leaving Pr atoms to reach Co($3d$)-O($2p$) bonds. The charge-transfer process extends over the interval 61–100 K in Fig. 3(b).

So, XAS data reveal that the strong Pr-O bond contraction detected at T_{MI} by neutron diffraction is due to a significant overlap between the Pr $4f$ wave functions and selected oxygens that abruptly shift the Pr valence towards the tetravalent $4f^1$ state.[28] As the electrical neutrality requires, Co L_3 XAS spectra of $Pr_{0.5}Ca_{0.5}CoO_3$ confirm that the electronic migration from Pr is compensated by changes in the Co valence. Co L_3 XAS spectra recorded by using the ALICE diffractometer chamber[29] on PM-3 are shown in Fig. 4 as a function of temperature. Important modifications show up at this edge coinciding with the transition. As a guide for the valence states of Co ions, the changes in Fig. 4 are compared to the reference compounds $SrCoO_3$ (Co^{4+}) and $AgCoO_2$ (Co^{3+}) (from Ref. 30). The spectra of these formally tetravalent and trivalent systems at RT mainly differ in the intensity of the shoulder at 2eV below the main peak. A clear loss of intensity in the shoulder at ~780.7 eV (2 eV below the maximum) has been detected at the MIT in $Pr_{0.5}Ca_{0.5}CoO_3$ as expected from a charge transfer from Pr to Co sites. Outside the temperature window of the transition the spectra shown in Fig. 4 hardly change.

Figure 5 shows the temperature dependence of the Co L_3-edge FY-XAS intensity measured at 780.7 eV, where the largest specific contribution from Co^{4+} valence is expected.[30] For comparison the figure also depicts the evolution of the valence shift inferred from Pr L_3-edge data. From this plot it is apparent that the T dependence of the Co L_3-edge feature follows exactly the T dependence of the Pr valence confirming an identical origin. Moreover, the sudden strong decrease of the Co intensity on cooling consistently agrees with a substantial

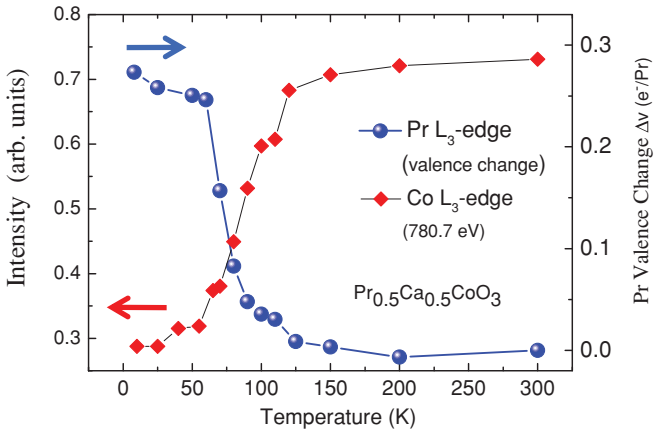

FIG. 5. (Color online) Temperature dependence of the Co L_3-edge FY-XAS intensity at 780.7 eV [larger contribution for Co^{4+} than for Co^{3+} (Ref. 30)]. The evolution is compared with the estimated Pr valence shift as deduced from Pr L_3-edge data in the same $Pr_{0.5}Ca_{0.5}CoO_3$ sample.

valence shift in Co sites towards the Co^{3+} t_{2g}^6 electronic state.

Neutron diffraction data and XAS spectra are thus consistent and indicate that the average valence of cobalt should decrease approaching the trivalent state. Moreover, the Co^{3+} IS state and the HS (high spin) are not favored in the low-temperature phase because the smaller cell volume favors enhanced crystal-field splitting between e_g and t_{2g} orbitals.[31] As a result, the detected transfer of charges in $Pr_{0.5}Ca_{0.5}CoO_3$ should correspond to $\frac{1}{2}$ [Pr]$4f^2$ + $\frac{1}{2}$ [Co]$t_{2g}^5 e_g^1$ + $\frac{1}{2}$ [Co]t_{2g}^5 $\rightarrow$ $\frac{1}{2}$ [Pr]$4f^1$ + [Co]t_{2g}^6 per formula unit (f. u.). Namely, there is a stabilization of the trivalent LS state of Co in the localized phase induced by a destabilization of the trivalent valence state of praseodymium. According to Fig. 3(a), electron migration is only partial: $\frac{1}{2}$ Pr^{3+} + $Co^{3.5}$ $\rightarrow$ $\frac{1}{2}$ $Pr^{3+2\delta}$ + $Co^{3.5-\delta}$, with $2\delta = \Delta v[\mathrm{Pr}] \approx 0.26e^-$. The drop in the susceptibility below T_{MI} is mainly a signature of the stabilization of the t_{2g}^6 state at Co^{3+} sites (LS), but it is also due to a reduction of the moment at Pr sites.

The present experimental results nicely agree with the electronic-structure calculations by Kníže k *et al.* in Ref. 14. They predicted a reduction of $t_{2g}^5(\sigma^*)^{0.5}$ states around the Fermi level, and their substitution at the critical temperature by a narrow Pr 4*f* band.[14] They anticipated that the gap could be associated to a charge transfer between the Pr and Co sites. Absorption data across the Pr L_3 edge are consistent with the energy of Pr 4*f* bands being relatively near the Fermi level in the metallic state, and a part of them becoming unoccupied and shifted above E_F below T_{MI}. Simultaneously, concomitant with the gap opening, some initially empty Co t_{2g} symmetry states move below Fermi level being occupied by electrons originally in states of *f* symmetry. The result is a charge transfer from Pr-4*f* to Co-3*d*-t_{2g} states at T_{MI} on cooling.

IV. CONCLUSION

In summary, x-ray absorption spectroscopy measurements in $Pr_{0.5}Ca_{0.5}CoO_3$ and $(Pr,Y)_{0.55}Ca_{0.45}CoO_3$ compositions reveal that the valence of praseodymium ions is stable and essentially +3 (Pr [$4f^2$]) in the metallic state, but abruptly increases approaching the oxidation state +4 (Pr [$4f^1$]) at the MIT transition. This mechanism appears to be the driving force of the metal-insulator transition. Moreover, the tilting ϕ_1 of CoO_6 octahedra is found to play a prominent role in the occurrence of the valence change and the concomitant electron localization.

Electrons leaving Pr sites are used to stabilize the trivalent low-spin state of Co. The ground state at low temperature is not realized through segregation of low- or intermediate-spin Co^{3+} and low-spin Co^{4+} ionic species. Instead, the $t_{2g}^5(\sigma^*)^{0.5}$ metallic state is substituted by a homogeneous $Co^{3.5-\delta}$ state stabilized by electron transfer from praseodymium: $\frac{1}{2}$ Pr^{3+} + $Co^{3.5}$ $\rightarrow$ $\frac{1}{2}$ $Pr^{3+2\delta}$ + $Co^{3.5-\delta}$, with $2\delta \approx 0.26e^-$ in $Pr_{0.5}Ca_{0.5}CoO_3$.

Note added: Recently, we became aware of a paper by J. Hejtmánek *et al.*[32] in which the Schottky peak in the specific heat of $(Pr,Y)_{0.7}Ca_{0.3}CoO_3$ samples is studied. The result indicates that the present conclusions also apply to lower Ca dopings.

ACKNOWLEDGMENTS

Financial support from MICINN (Spanish government) under Projects No. MAT2006-11080-C02-02 and No. MAT2009-09308, and NANOSELECT under Project No. CSD2007-00041 is acknowledged. We thank ILL (and the CRG-D1B), and HZB for the provision of beam time. The authors gratefully acknowledge C. Ritter for his assistance with neutron data collection. The ALICE diffractometer is funded through the BMBF under Contract No. 05KS7PC1. The research leading to these results has received funding from the European Community's Seventh Framework Programme (FP7/2007-2013) under grant agreement No. 226716.

*garcia.munoz@icmab.es

[1] Z. Shao and S. M. Haile, Nature (London) **431**, 170 (2004).
[2] Y. Wang, N. S. Rogado, R. J. Cava, and N. P. Ong, Nature (London) **423**, 425 (2003).
[3] W. Kobayashi, S. Ishiwata, I. Terasaki, M. Takano, I. Grigoraviciute, H. Yamauchi, and M. Karppinen, Phys. Rev. B **72**, 104408 (2005).
[4] I. O. Troyanchuk, N. V. Kasper, D. D. Khalyavin, H. Szymczak, R. Szymczak, and M. Baran, Phys. Rev. Lett. **80**, 3380 (1998).
[5] K. Takada, H. Sakurai, E. Takyama-Muromachi, F. Izumi, R. A. Dilanian, and T. Sasaki, Nature (London) **422**, 53 (2003).
[6] J. B. Goodenough, J. Phys. Chem. Solids **6**, 287 (1958).
[7] M. A. Señarís-Rodríguez and J. B. Goodenough, J. Solid State Chem. **116**, 224 (1995).

[8]T. Saitoh, T. Mizokawa, A. Fujimori, M. Abbate, Y. Takeda, and M. Takano, Phys. Rev. B **55**, 4257 (1997).
[9]P. G. Radaelli and S.-W. Cheong, Phys. Rev. B **66**, 094408 (2002).
[10]K. Knížek, P. Novák, and Z. Jirák, Phys. Rev. B **71**, 054420 (2005).
[11]C. Frontera, J. L. García-Muñoz, A. Llobet, and M. A. G. Aranda, Phys. Rev. B **65**, 180405(R) (2002).
[12]S. Tsubouchi, T. Kyômen, M. Itoh, P. Ganguly, M. Oguni, Y. Shimojo, Y. Morii, and Y. Ishii, Phys. Rev. B **66**, 052418 (2002).
[13]A. Maignan, V. Caignaert, B. Raveau, D. Khomskii, and G. Sawatzky, Phys. Rev. Lett. **93**, 026401 (2004).
[14]K. Knížek, J. Hejtmánek, P. Novák, and Z. Jirák, Phys. Rev. B **81**, 155113 (2010).
[15]Y. Okimoto, X. Peng, M. Tamura, T. Morita, K. Onda, T. Ishikawa, S. Koshihara, N. Todoroki, T. Kyomen, and M. Itoh, Phys. Rev. Lett. **103**, 027402 (2009).
[16]S. Tsubouchi, T. Kyômen, M. Itoh, and M. Oguni, Phys. Rev. B **69**, 144406 (2004).
[17]T. Fujita, T. Miyashita, Y. Yasui, Y. Kobayashi, M. Sato, E. Nishibori, M. Sakata, Y. Shimojo, N. Igawa, Y. Ishii, K. Kakurai, T. Adachi, Y. Ohishi, and M. Takata, J. Phys. Soc. Jpn. **73**, 1987 (2004).
[18]T. Fujita, S. Kawabata, M. Sato, N. Kurita, M. Hedo, and Y. Uwatoko, J. Phys. Soc. Jpn. **74**, 2294 (2005).
[19]H. Masuda, T. Fujita, T. Miyashita, M. Soda, Y. Yasui, Y. Kobayashi, and M. Sato, J. Phys. Soc. Jpn. **72**, 873 (2003).
[20]A. J. Barón-González, C. Frontera, J. L. García-Muñoz, J. Blasco, and C. Ritter, Phys. Rev. B **81**, 054427 (2010).
[21]A. Chichev, J. Hejtmánek, Z. Jirák, K. Knížek, M. Maryško, M. Dlouhá, and S. Vratislav, J. Magn. Magn. Mater. **316**, e728 (2007).
[22]P. Tong, Y. Wu, B. Kim, D. Kwon, J. M. S. Park, and B. G. Kim, J. Phys. Soc. Jpn. **78**, 034702 (2009).
[23]E. Dudzik, R. Feyerherm, W. Diete, R. Signorato, and C. Zilkens, J. Synchrotron Radiat. **13**, 421 (2006).
[24]A. Bianconi, A. Marcelli, H. Dexpert, R. Karnatak, A. Kotani, T. Jo, and J. Petiau, Phys. Rev. B **35**, 806 (1987).
[25]H. Yamaoka, H. Oohashi, I. Jarrige, T. Terashima, Y. Zou, H. Mizota, S. Sakakura, T. Tochio, Y. Ito, E. Ya. Sherman, and A. Kotani, Phys. Rev. B **77**, 045135 (2008).
[26]J. Richter, A. Braun, A. S. Harvey, P. Holtappels, T. Graule, and L. J. Gauckler, Physica B **403**, 87 (2008).
[27]W. Xu, A. Marcelli, B. Joseph, A. Iadecola, W. S. Chu, D. Di Gioacchino, A. Bianconi, Z. Y. Wu, and N. L. Saini, J. Phys.: Condens. Matter **22**, 125701 (2010).
[28]The tetravalent state of Pr signaled by feature *B* was also recognized at Pr-$M_{4,5}$ edges below the transition (paper in preparation).
[29]J. Grabis, A. Nefedov, and H. Zabel, Rev. Sci. Instrum. **74**, 4048 (2003).
[30]S. S. Lee, J. H. Kim, S. C. Wi, G. Kim, J.-S. Kang, Y. J. Shin, S. W. Han, K. H. Kim, H. J. Song, and H. J. Shin, J. Appl. Phys. **97**, 10A309 (2005); R. H. Potze, G. A. Sawatzky, and M. Abbate, **51**, 11501 (1995).
[31]J.-Q. Yan, J.-S. Zhou, and J. B. Goodenough, Phys. Rev. B **69**, 134409 (2004).
[32]J. Hejtmánek *et al.*, Phys. Rev. B **82**, 165107 (2010).